

CONTACT ANGLE MEASUREMENT OF WOOD FIBERS IN SURFACTANT AND POLYMER SOLUTIONS

Yulin Deng

Assistant Professor

and

Marcos Abazeri

Assistant Engineer

Institute of Paper Science and Technology
500 10th Street, N.W., Atlanta, GA 30318

(Received August 1997)

ABSTRACT

The Wilhelmy principle was used to investigate the wettability of wood fibers in various aqueous solutions. The sensitivity and reproducibility of the measurement were significantly improved by using a group of separated fibers as compared to a single-fiber method that was reported previously. This accurate and reproducible method allowed us to investigate contact angle and wettability of wood fibers in aqueous solutions using a common dynamic contact angle analyzer without the interference of capillary and roughness from the paper sheet surface.

The wettability of different solutions on various wood fibers, including bleached and unbleached, and AKD (alkyl ketene dimer) sized and unsized fibers, was studied. The results indicated that the receding contact angle of aqueous solution against wood fibers is zero or close to zero regardless of the nature of the wood fiber surface. However, the advancing contact angle of aqueous solution against wood fibers strongly depends on the fiber surface properties.

A decrease in advancing contact angle with an increase of the surfactant concentration was observed for all types of surfactants and fibers used in this study. The water-soluble cationic polyDADMAC [poly(diallyldimethylammonium chloride)] and nonionic PEO (polyethylene oxide) have no significant effect on the wettability of wood fibers in aqueous solutions.

Keywords: Contact angle, hydrophobic, wood fiber, wettability, surfactant, polymer, adsorption.

INTRODUCTION

The contact angle of aqueous solutions on a wood fiber surface is very important for papermaking, paper printing, and recycling. However, the methods that can be used for contact angle measurement of small wood fibers in liquid are limited. The results obtained from wettability measurement by using a paper sheet may lead to a misunderstanding because of the interference of porous structure and surface roughness of a paper sheet. It is important for papermakers to know the surface properties of individual fibers rather than that of paper sheets in some cases because the fibers in pulp suspension are separately suspended in water. The surface chemistry of the

individual fibers is also important for the paper recycling industry. For example, the fiber-ink and fiber-air bubble interactions in a flotation deinking cell will strongly depend on the surface chemistry of individual fibers.

It has been well known that the adsorption and orientation of surfactant or polymer molecules on the matrixes will significantly affect the hydrophobicity of a solid surface. In a recent study of fiber fractionation by using a flotation technique, it has been found (Li and Muvundamina 1994, 1995) that long fibers float more easily than pulp fines. To explain this phenomenon, Li and Muvundamina (1994) assumed that surfactant molecules have different orientations on fines and fibers. The

surface of fines is more hydrophobic than long fibers because of its high lignin content. When surfactants adsorb on fines, the hydrophobic tails of surfactant anchor onto hydrophobic sites of fines and leave the charged heads (or hydrophilic parts) toward the water phase. This leads to an increase of hydrophilicity of the surface of fines and prevents them from adhering onto air bubble surfaces. For long fibers, on the other hand, the surface is very hydrophilic, and surfactant adsorption is through the interaction between hydroxyl groups of fiber surface and charged heads of surfactant molecules (or hydrophilic parts of nonionic surfactant). However, no direct contact angle data support this assumption.

It is difficult to measure the contact angle of liquid on individual wood fibers because the fiber length is too small to be handled, and the wetting force of a single fiber in solution is too small to be measured. The optical measurements of contact angles of liquids against fibers have been attempted by Foote (1939), Jones and Porter (1967), and Grindstaff (1969). However, the reproducibility of these methods is poor because it is difficult to measure accurately the contact angle of liquid on very small wood fibers using an optical technique. Furthermore, these methods yield only a single θ -value, which may be highly unrepresentative of the average properties of the fiber heterogeneity. A more satisfactory approach to the determination of fiber-liquid contact angles employs the Wilhelmy principle, in which the downward force upon a single fiber suspended vertically through the liquid surface is measured (Hodgson and Berg 1988; Krueger and Hodgson 1994, 1995). However, a poor reproducibility was observed when a single fiber was used because (1) the heterogeneity of wood fibers is high and the data obtained using a single fiber may be significantly different from the average value of a pulp furnish, and (2) the wetting force is too small, which results in a large uncertainty. Instead of using a single fiber, a technique using a group of separated fibers has been developed in this study, and the wettability of wood fi-

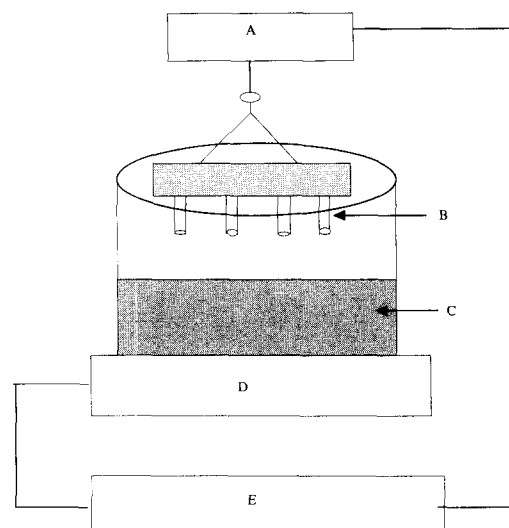


FIG. 1. Schematic diagram of dynamic wetting force measurement using fiber group technique; A: electronic microbalance, B: fibers, C: wetting liquid, D: traveling elevator system, and E: computer.

bers in different aqueous solutions has been studied.

EXPERIMENTAL

Surface tension and contact angle measurements

The surface tension of a liquid solution was measured by a dynamic contact angle analyzer (Cahn DCA 312) using a glass plate. The instrument used for contact angle measurement is shown schematically in Fig. 1.

In a previous study, Klungness (1996) found that the receding contact angle of water on wood fibers was zero, i.e. $\cos\theta_r = 1$, where θ_r is the receding contact angle. Hodgson and Berg (1988) and Krueger and Hodgson (1994, 1995) found that not only water but most aqueous solutions on wood fibers give receding contact angle of zero.

For an object immersed in a liquid, the dynamic wetting force can be written as

$$F = P\gamma\cos\theta - (\rho_l - \rho_g)V \quad (1)$$

where F is the force on the object; P is the wetted perimeter; γ is the surface tension of

TABLE 1. *Dry fiber properties.*

Fibers	Average length (mm)	Average perimeter of dry fiber (μm)	Fiber wall thickness of dry fiber (μm)	Average perimeter of dry fiber (μm)	Fiber wall thickness of dry fiber (μm)	Sizing
Bleached southern pine	2.83	102	4.95	115	7.42	No
0.2% AKD sized bleached southern pine	2.83	102	—	—	—	0.2% AKD
0.6% AKD sized bleached southern pine	2.83	102	—	—	—	0.6% AKD

liquid-air surface; θ is the contact angle of liquid on a solid surface; V is the submerged volume, and ρ_l and ρ_g are the liquid and air densities, respectively.

Because the buoyancy force is negligible compared to the total force for very small fibers (about 1% of total wetting force) (Hodgson and Berg 1988; Krueger and Hodgson 1994, 1995), the dynamic wetting force reduces to

$$F = P\gamma\cos\theta \quad (2)$$

However, using Eq. (2) to calculate the contact angle of wood fiber depends on the accurate value of the fiber perimeter. Although Young (1976) used a light microscope equipped with a calibrated eyepiece to measure the fiber perimeter, the swelling degree of fiber in liquid, the heterogeneity of the fiber perimeter along the fiber length, and the capillary effects from fiber surface roughness and hollow structure cannot be measured using a microscope. This leads to the following relationship

$$\cos\theta_A = F_A/F_R \quad (3)$$

where θ_A is the advancing contact angle; F_A and F_R are the advancing and receding dynamic wetting forces, respectively. Equation (3) suggests that an advancing contact angle can be obtained by advancing and receding forces without knowing the fiber perimeter.

Although Eq. (3) has been used to calculate the advancing contact angle of aqueous liquids on wood fibers, it is not clear whether the zero-receding contact angle assumption can be generally used for systems such as fiber in surfactant or polymer solutions, which are im-

portant for papermaking and recycling. In this study, the zero-receding contact angle assumption will be further verified using different surfactant solutions and fibers.

Although Hodgson and Berg (1988), Krueger and Hodgson (1994, 1995), and Klungness (1981) provided a very useful technique for determining the contact angle of liquid on a single fiber, a large experimental uncertainty was uncovered because the dynamic wetting force for a single fiber is too small. Furthermore, it is a general requirement that more than 10 independent samples have to be measured if a reliable value can be obtained because of the heterogeneity of wood fibers. These problems can be solved by a modified technique, which was developed in this study.

The liquid is contained in a 50-ml glass beaker that can be raised up and down by a traveling elevator system, which allows the liquid to advance or recede over the sample at a controlled rate (0.01 mm min^{-1}). One end of 4–7 individual fibers was separately stuck on the adhesive tape keeping the other end in a straight line (see Fig. 1). The ends of the fibers were carefully cut to the same level, if necessary. The distance between individual fibers was greater than 1 mm to avoid the effect of capillary force between two fibers. The dynamic wetting forces on the fibers was measured by an electronic microbalance (0.1 mg resolution) and analyzed by a computer using DCA software.

Materials

The fibers used in this study are given in Table 1. The fiber lengths were determined by

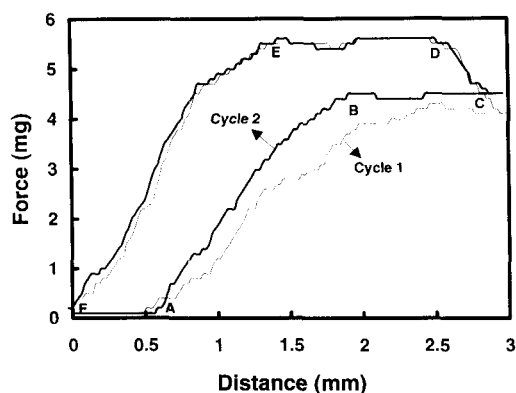


FIG. 2. The traces of dynamic wetting forces of distilled water on a group of 5 separated fibers.

image analysis. The width of fibers was measured using 400 \times magnification with the aid of OPTIMAS image analysis software. The sized fibers were made by the reaction of fibers with varying amounts of a cationic AKD sizing emulsion (Hercon 70, Hercules Inc.) in \sim 3% fiber consistency for 5 minutes. The furnishes were filtered and air-dried for 2 hours. The air-dried fibers were then heated to 100 $^{\circ}$ C in a vacuum oven for \sim 30 minutes.

Triton X-100 (analyze grade, J. T. Backer Inc.), cetyltrimethylammonium bromide [$\text{CH}_3(\text{CH}_2)_{15}\text{N}(\text{CH}_3)_3\text{Br}$, CTMAB, Aldrich, 95%], and sodium dodecylsulphate (SDS) (Specially pure, BDH Inc.) were used as non-ionic, cationic, and anionic surfactants, respectively. Poly(diallyldimethylammonium chloride) (polyDADMAC, Polysciences Inc., 15% solid) was used as a water-soluble cationic polyelectrolyte. The charge density of the polymer, determined by colloid titration, was 7.075 meq/g. Poly(ethylene oxide) (PEO, 10,000 g/mol, Aldrich) was used as a non-ionic polymer. All of the surfactants and polymers were used as received.

RESULTS AND DISCUSSION

The typical curves of receding and advancing dynamic wetting forces measured using a group of separated fibers are shown in Fig. 2. During the measurement, the fibers were immersed in (advancing) or pulled out (receding)

of the liquid at a constant velocity. When the fibers were immersed into the liquid, a trace of the advancing force was recorded from **A** to **B**. It was noted that the advancing wetting force obtained by a group of separated fibers increases very slowly with the immersed distance, which is significantly different from the trace of wetting force obtained by a glass plate in the same liquid, i.e., a sharp increase in the wetting force is usually observed when a glass plate is immersing into the liquid. Several factors may slow the increase of advancing wetting force of wood fibers. First, the fibers were gradually swelled when dry fibers are immersed into an aqueous solution. Because the fiber swelling will result in an increase in the fiber perimeter, the dynamic wetting force must gradually increase. Second, the wood fibers are heterogeneous along the fiber length. The heterogeneity of the fiber perimeter along its length (needle-like shape) is easy to see under a microscope, which must result in a gradual increase in the fiber wetting force when fibers are immersed into the liquids. Furthermore, the fibers may not attach to the liquid surface simultaneously, which results in an increase in the wetting force when more fibers are immersed into the liquid.

As the fibers were immersed further from **B** to **C**, a constant advancing force was recorded. The trace of wetting force from **B** to **C** is also different from the trace of water over a glass plate. For a glass immersing into water, the wetting force decreases with submerged volume because of the increase of buoyancy force; but a constant force was obtained when wood fibers were used instead of a glass plate. It is well known that in order to calculate a contact angle using the Wilhelmy principle, it is necessary to extrapolate the dynamic wetting force to zero-submerged volume to eliminate the buoyancy force. However, it is difficult to detect where the zero-submerged volume is if a group of separated fibers is used because all fibers may not attach to the liquid surface simultaneously. Fortunately, as discussed before, the buoyancy force obtained from a group of separated fibers may be neg-

ligible compared to the total wetting force, which suggests that it is not necessary to extrapolate the dynamic wetting force to zero contact point. This is confirmed by Fig. 2, which shows that the wetting force is independent of the submerged volume of fibers from **B** to **C**.

Comparing the calculated buoyancy force to the total wetting force shown in Fig. 2, it was found that the maximum buoyancy force of wood fibers in water was only ~1% of the total wetting force. This suggests that the total advancing wetting force of wood fibers in a solution can be directly obtained from **B** to **C** without any correction to the submerged volume. A similar conclusion can also be expected for the receding force. In this study, the stable dynamic wetting forces (**B** to **C** for advancing, and **D** to **E** for receding) were directly used to calculate the contact angles.

After fibers reached the maximum depth at **C**, they were gradually pulled out from the liquid until reaching position **D**, at which a stable receding force was obtained. The receding force remained constant from **D** to **E** and then decreased from **E** to **F** where the fibers were totally pulled out from the liquid.

The dependence of the total force on the wetting time was observed in this study. It can be seen from Fig. 2 that the advancing force of the first cycle is smaller than that of the second, but the receding force is the same for the first and second cycles. This is not surprising because the advancing wetting force was obtained from dry fibers for the first cycle, but from wet fibers for the second cycle. Obviously, dry fibers have different perimeter and surface properties from wet fibers. After the first cycle, the fibers were wet and both the fiber perimeter and the wetting forces reached an equilibrium value. For the receding force, the fibers were always wet regardless of whether it was in the first or the second cycle. The difference in advancing contact angles between the first and the second cycles was observed for all of the fibers and the solutions, such as bleached fibers and sized fibers in TX-100 solutions, and unbleached hardwood fi-

bers in different surfactant solutions. After fibers were wet, stable wetting forces were obtained for both advancing and receding processes. All of the measurements made in this study were reproducible with an experimental error of less than $\pm 8\%$.

Verification of zero-receding contact angle

Although it was indicated in previous studies (Klungness 1981; Hodgson and Berg 1988) that the receding contact angle of water over a single wood fiber is zero, further experimental proofs are needed, particularly for the sized fibers in a surfactant or polymer solution.

For the same fibers in different solutions (surfactant, polymer, etc.), Eq. (2) gives the following relationships:

$$\begin{aligned}\frac{F_R^1}{\gamma^1} &= p \cos\theta_R^1 \\ \frac{F_R^2}{\gamma^2} &= p \cos\theta_R^2 \\ &\dots \\ \frac{F_R^n}{\gamma^n} &= p \cos\theta_R^n\end{aligned}\quad (4)$$

where the superscriptions 1, 2, and n represent the different solutions. If the zero-receding contact angle assumption can be used for the same fibers in different solutions, Eq. (4) can be rewritten as

$$\frac{F_R^1}{\gamma^1} = \frac{F_R^2}{\gamma^2} = \dots = \frac{F_R^n}{\gamma^n} = p \quad (5)$$

Equation (5) indicates that, if the receding contact angle is really zero, the force ratio (F_R^n/γ^n) must be a constant that equals the perimeter P of the fibers. In contrast, if the receding contact angle is not zero, F_R^n/γ^n must be a function of $\cos\theta_R$ and surface tension γ .

Figure 3 shows the wetting forces of a group of separated fibers as a function of TX-100 concentration. It can be seen that although the surface tension of TX-100 decreases as the surfactant concentration increases up to 190 mg/L (the critical micellization concentration

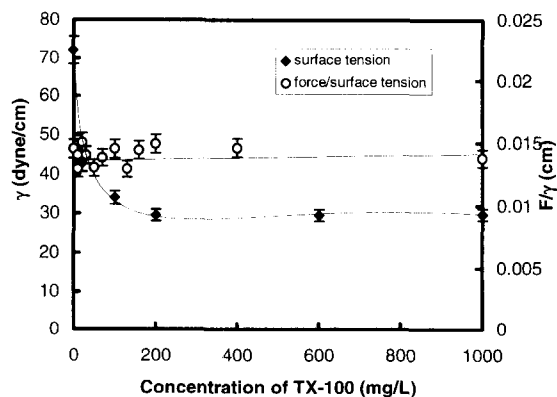


FIG. 3. Surface tension γ and force ratio F_R/γ as a function of TX-100 concentration at room temperature for bleached southern pine fibers.

of TX-100), the values of F_R/γ^n can be described well by Eq. (5) under experimental uncertainty. This strongly suggests that although the surface chemistry of the fibers may be different in these solutions because of the adsorption of surfactant, the receding contact angle of aqueous solutions on these wood fibers is always equal to zero. The zero-receding contact angle assumption was further verified using different types of surfactants and polymers, such as cationic surfactant (CTMAB), anionic surfactant (SDS), and cationic polymer polyDADMAC. The value of F_R/γ^n in different surfactant and polymer solutions as a function of surface tension is given in Fig. 4. Surprisingly, the receding contact angle of bleached southern pine fibers in all aqueous solutions is zero or close to zero although the adsorption and the orientation of different chemicals may significantly change the fiber surface properties. The uncertainty of the receding contact angle measured in this study will be discussed later.

The perimeter of $145 \pm 9 \mu\text{m}$ for a single fiber was obtained from the data shown in Fig. 3 using Eq. (5). This value is 1.42 times the perimeter of dry fibers and 1.25 times that of wet fibers obtained by image analysis. The difference in the diameters obtained from the Wilhelmy principle and that from image analysis may suggest that the perimeter calculated

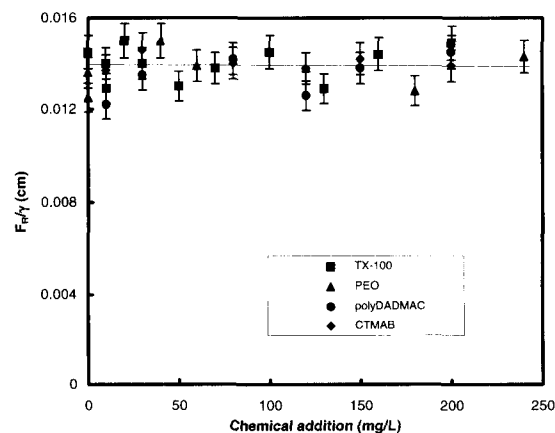


FIG. 4. Force ratio F_R/γ as a function of chemical concentrations of nonionic surfactant TX-100, cationic surfactant CTMAB, cationic polymer polyDADMAC, and nonionic polymer PEO. Fibers: bleached southern pine fibers.

from Eq. (5) is only an apparent perimeter, and the lumen structure and surface roughness of the fiber may also affect the total force F_R .

The receding wetting force and contact angle of 0.6% AKD sized fibers in TX-100 solution were also examined using Eq. (5). Because AKD is very hydrophobic, the sized fibers used in force measurements must be stiff enough to resist bending when fibers are immersed in the liquids. Furthermore, because the advancing wetting force may be very small, even negative, when highly sized fibers are used, the electronic microbalance must be sensitive enough. These limitations make the measurements more difficult and lead to a higher experimental uncertainty. However, after several repeated measurements, it was found that when a surfactant was added into the liquid, both the hydrophobicity of sized fibers and the surface tension of the liquid decreased so that the fibers could be easily immersed into the liquid without bending. It was also noted that, in a pure water system, although the sizing materials significantly decrease the advancing force of fibers, they almost do not impact the receding force. This interesting behavior is shown in Fig. 5.

The receding forces obtained from 0.6%

